

Franck-Condon-Broadened Angle-Resolved Photoemission Spectra Predicted in LaMnO₃

Vasili Perebeinos and Philip B. Allen

Department of Physics and Astronomy, State University of New York, Stony Brook, NY 11794-3800
(November 1, 2018)

The sudden photohole of least energy created in the photoemission process is a vibrationally excited state of a small polaron. Therefore the photoemission spectrum in LaMnO₃ is predicted to have multiple Franck-Condon vibrational sidebands. This generates an intrinsic line broadening ≈ 0.5 eV. The photoemission spectral function has two peaks whose central energies disperse with band width ≈ 1.2 eV. Signatures of these phenomena are predicted to appear in angle-resolved photoemission spectra.

79.60.-i, 71.38+i, 75.30.Vn

The colossal magnetoresistance (CMR) effect [1] in doped manganese oxides has attracted a lot of attention. The interplay of charge, orbital and magnetic order results in a very rich phase diagram [2]. The parent compound LaMnO₃ has orthorhombic symmetry at low temperature. The Mn³⁺ ion has d^4 (t_{2g}^3, e_g^1) configuration with an “inert” t_{2g} core (spin 3/2) and a half-filled doubly degenerate e_g -type d orbital which is Jahn-Teller (JT) unstable. Ignoring rotation of the MnO₆ octahedra, which occurs below 1010 K, the JT symmetry breaking is cubic to tetragonal [3] at $T_{JT} = 750$ K. The corresponding orbital order [4] has x - and y -oriented E_g orbitals alternating in the $x - y$ plane with wave vector $\vec{Q} = (\pi, \pi, 0)$. This in turn causes layered antiferromagnetic (AFA) order to set in at $T_N = 140$ K.

The electronic structure of LaMnO₃ has been studied, for example, by photoemission [5,6] and by first principles calculations [7]. Still there is controversy about the nature of the low energy excitations, arising from the interplay between strong on-site Coulomb repulsion (which leads to magnetic order) and strong electron-phonon (e-p) interactions [8] (which lead to orbital order).

When an electron is removed from the JT-ordered ground state, e-p coupling causes the hole to self-localize in an “anti-JT” small polaron state. In a previous paper [9] we have described the localized polaron in adiabatic approximation. Residual non-adiabatic coupling allows the hole to disperse with band width narrowed by Huang-Rhys factor $e^{-3\Delta/4\hbar\omega} \approx 10^{-4}$. The photoemission process is sudden. The emitted electron with wavevector \vec{k} leaves a hole in a lattice “frozen” in the unrelaxed JT state. Ignoring lattice relaxation, this hole would disperse with band width $2t \approx 1$ eV (t is the hopping parameter), as shown on Fig. 1. However, this is not a stationary state and must be regarded as a superposition of exponentially narrowed small polaron bands. Such bands have anti-JT oxygen distortions at each site, but a sufficient number of vibrational quanta are also excited such that the anti-JT distortion at time zero is “undone”. This is “Franck-Condon principle”.

The measured spectrum at wavevector \vec{k} will consist of a central δ -function at the energy of the frozen lattice (dispersive) band $\varepsilon_{1,2}(\vec{k})$, plus multiple vibrational sidebands at energy $\varepsilon_{1,2}(\vec{k}) \pm n\hbar\omega$, with an overall Gaussian envelope whose width is approximately the polaron binding energy. Franck-Condon broadening has been seen in photoemission spectra of solid nitrogen and oxygen [10].

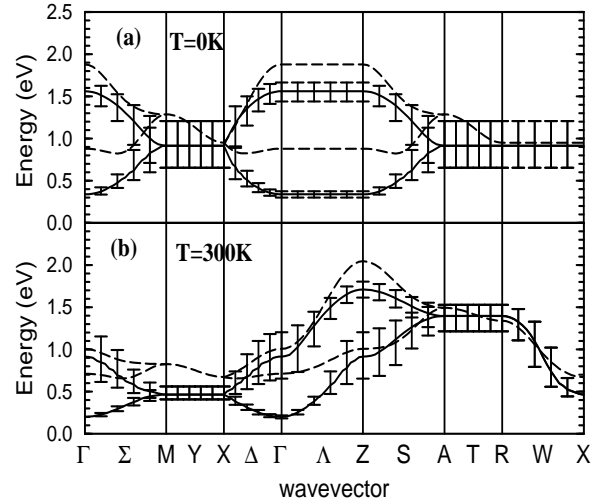


FIG. 1. Peak positions of the ARPES (a) at $T=0$ K and (b) at $T=300$ K along high-symmetry lines of the tetragonal Brillouin zone are shown by solid lines. Spin disorder at T above the Neel temperature T_N effectively reduces the hopping parameter $t=(dd\sigma)$ by 2/3 and adds hopping in \hat{z} direction which strongly affects dispersion. Error bars (FWHM of the photoemission peak) represent Franck-Condon broadening. Band structure ($U=0$ limit) peak positions $\lambda_{1,2}(\vec{k})$ are shown by dashed lines.

We find at each wavevector \vec{k} the photoemission spectrum has an intrinsic Franck-Condon broadening indicated by error bars in Fig. 1. The position of the maximum disperses with \vec{k} -vector close to the “frozen” lattice spectrum. A qualitative picture of this process has been given by Sawatzky [11] in the context of high temper-

ature superconductors and by Dessau and Shen [6] for the manganites. The present paper gives an exact algebraic prediction for the Angle-Resolved-Photoemission-Spectra (ARPES) of a model Hamiltonian for LaMnO₃.

Our model Hamiltonian [9], first introduced by Millis [12], has hopping \mathcal{H}_{el} , electron-phonon \mathcal{H}_{ep} , and lattice \mathcal{H}_{L} energies:

$$\begin{aligned}\mathcal{H}_{\text{el}} &= t \sum_{\ell, \pm} \{ [c_x^\dagger(\ell) c_x(\ell \pm \hat{x})] + [x \rightarrow y] + [y \rightarrow z] \} \\ \mathcal{H}_{\text{ep}} &= -g \sum_{\ell, \alpha} \hat{n}_{\ell, \alpha} (u_{\ell, \alpha} - u_{\ell, -\alpha}) \\ \mathcal{H}_{\text{L}} &= \sum_{\ell, \alpha} (P_{\ell, \alpha}^2 / 2M + K u_{\ell, \alpha}^2 / 2).\end{aligned}\quad (1)$$

In these formulas $c_\alpha^\dagger(\ell)$ creates a state with orbital $\psi_\alpha = |3\alpha^2 - r^2\rangle$, where $\alpha = x, y, z$. These three orbitals span the two dimensional e_g subspace and can be expressed in terms of the conventional orthogonal basis $\Psi_2 = d_{x^2-y^2}$, $\Psi_3 = d_{3z^2-r^2} = \Psi_z$; specifically $\Psi_{x,y} = \pm\sqrt{3}/2\Psi_2 - \Psi_3/2$. The resulting \mathcal{H}_{el} coincides with the nearest-neighbor two-center Slater-Koster [13] hopping Hamiltonian with overlap integral $t = (dd\sigma)$ and $(dd\delta) = 0$. The hopping parameter $t = 0.5$ eV is chosen to agree with an *ab initio* e_g band width of 1 eV [7]. The e-p interaction \mathcal{H}_{ep} is modeled by a linear energy reduction of an occupied ψ_x orbital ($\hat{n}_{\ell, x} = c_x^\dagger(\ell) c_x(\ell)$) if the corresponding two oxygens in the $\pm\hat{x}$ direction expand outwards, and similarly for \hat{y} and \hat{z} oxygens if ψ_y or ψ_z orbitals are occupied. The strength of the e-p coupling g determines the JT splitting $2\Delta = 1.9$ eV, which is fitted to agree with the lowest optical conductivity peak [14,15]. Static oxygen distortions $2u = \sqrt{2\Delta/M\omega^2} = 0.296$ Å given by our model agree well with neutron diffraction data 0.271 Å [3]. For the lattice term \mathcal{H}_{L} we use a simplified model where oxygen vibrations along Mn-O-Mn bonds are local Einstein oscillators. The displacement $u_{\ell, \alpha}$ is measured from cubic perovskite position of the nearest oxygen in the $\hat{\alpha}$ -direction to the Mn atom at ℓ . The oxygen vibrational energy $\hbar\omega = \hbar\sqrt{K/M} = 0.075$ eV is taken from Raman data [16]. In addition there is a large on-site Coulomb repulsion U and a large Hund energy. These terms inhibit hopping except to empty sites where the t_{2g} core spins are aligned correctly.

In adiabatic approximation one can solve this problem for $U=0$ or $U=\infty$. Both cases give a good description of the observed cooperative JT order. When $U=0$, the ground state wavefunction is:

$$|\text{GS}, 0\rangle = \prod_{\vec{k}} c_{\vec{k}1}^\dagger c_{\vec{k}2}^\dagger |\text{vac}\rangle. \quad (2)$$

A JT gap $\approx 2\Delta$ opens and the lower two bands of energy $\lambda_{\vec{k}1}$, $\lambda_{\vec{k}2}$ are filled. The photohole as initially created has energy:

$$\begin{aligned}\lambda_{1,2}^2 &= \Delta^2 + t^2(2C_x^2 + C_x C_y + 2C_y^2) \pm t|C_x + C_y| \\ &\quad \sqrt{\Delta^2 + 4t^2(C_x^2 - C_x C_y + C_y^2)},\end{aligned}\quad (3)$$

where $C_{x,y} = \cos k_{x,y}$ and C_z not entering at $T=0$ K. These bands are shown in Fig. 1(a) as dashed lines.

At this point, at least in principle, could proceed numerically to find the polaronic energy lowering. However, it is both easier and more realistic to switch to $U=\infty$. The ground state wavefunction:

$$|\text{GS}, \infty\rangle = \prod_{\ell} c_X^\dagger(\ell) \prod_{\ell'} c_Y^\dagger(\ell') |\text{vac}\rangle, \quad (4)$$

has orbitals $\Psi_{X,Y} = -(\Psi_3 \mp \Psi_2)/\sqrt{2}$ occupied singly on interpenetrating A and B sublattices. This is a fully correlated state with zero double occupancy, while Eq. (2) is a band wavefunction in which two electrons are found on the same Mn atom with non-zero probability. For $U \geq 6t \approx 3$ eV, the state (4) has lower energy than state (2) [9]. Neglecting creation of orbital defects with energy $\approx 2\Delta$ the “frozen” lattice approximation predicts photohole energies $\Delta + \varepsilon_{1,2}(\vec{k})$, where $\varepsilon_{1,2}(\vec{k}) = \pm(t/2)(C_x + C_y)$. We need to add a non-adiabatic treatment of the e-p coupling. The effective Hamiltonian $\mathcal{H}_{\text{eff}} = \mathcal{H}_{\text{el}} + \mathcal{H}_{\text{ep}} + \mathcal{H}_{\text{L}}$ for the single hole is:

$$\begin{aligned}\mathcal{H}_{\text{el}}^A &= \sum_{\ell \in A} \frac{t}{4} (d_Y^\dagger(\ell \pm x) d_X(\ell) + d_Y^\dagger(\ell \pm y) d_X(\ell)) \\ \mathcal{H}_{\text{ep}}^A + \mathcal{H}_{\text{L}}^A &= \sum_{\ell \in A} d_X^\dagger(\ell) d_X(\ell) \left[\Delta + \sum_{\alpha} \kappa_{\alpha} (a_{\alpha}(\ell) + \right. \\ &\quad \left. a_{\alpha}^\dagger(\ell) - b_{\alpha}(\ell - \alpha) - b_{\alpha}^\dagger(\ell - \alpha)) \right] + \sum_{\alpha} a_{\alpha}^\dagger(\ell) a_{\alpha}(\ell).\end{aligned}\quad (5)$$

Here the operator $d_X^\dagger(\ell) = c_X(\ell)$ creates a hole in the JT ground state by destroying an electron on orbital X at site ℓ (if $\ell \in A$ sublattice), and the operator $d_Y^\dagger(\ell) = c_Y(\ell)$ creates a hole on B sublattice (if $\ell \in B$). The phonon operators $a_{\alpha}^\dagger(\ell)$ or $b_{\alpha}^\dagger(\ell)$ create vibrational quanta on the $\ell + \hat{\alpha}/2$ oxygen, if $\ell \in A$ or $\ell \in B$ respectively. The e-p coupling constants are $\kappa_{x,y,z} = \sqrt{\Delta/12}(1 + \sqrt{3}/2; 1 - \sqrt{3}/2; 1)$. The Hamiltonian and all other energy parameters Δ and t in Eq. 5 are in units of $\hbar\omega$. The total Hamiltonian has an additional term $\mathcal{H}_{\text{el}}^B + \mathcal{H}_{\text{ep}}^B + \mathcal{H}_{\text{L}}^B$ which is obtained from Eq. (5) by interchanging operators:

$$d_Y \leftrightarrow d_X, a_x \leftrightarrow b_y, a_y \leftrightarrow b_x, a_z \leftrightarrow b_z \quad (6)$$

and summing over the B sublattice.

Following Cho and Toyozawa [17] we are able to diagonalize Hamiltonian (5) in a very large truncated basis of functions with a hole present on site ℓ and an arbitrary number of vibrational quanta $p_{\pm x}, p_{\pm y}, p_{\pm z}$ on the six displaced neighboring oxygens:

$$|\Psi^A(\ell, \{p\})\rangle = d_{X'}^\dagger(\ell) \prod_{\alpha} U_{\ell}^{a_{\alpha}}(-\kappa_{\alpha}) \frac{(a_{\alpha}^{\dagger}(\ell))^{p+\alpha}}{\sqrt{p+\alpha!}} U_{\ell-\alpha}^{b_{\alpha}}(\kappa_{\alpha}) \frac{(b_{\alpha}^{\dagger}(\ell-\alpha))^{p-\alpha}}{\sqrt{p-\alpha!}} |\text{GS}, \infty\rangle. \quad (7)$$

The displacement operator $U_{\ell}^a(\kappa) = \exp[-\kappa(a_{\ell} - a_{\ell}^{\dagger})]$ makes the $\mathcal{H}_{\text{ep}} + \mathcal{H}_{\text{L}}$ part of the Hamiltonian diagonal. To get basis functions $|\Psi^B(\ell, \{p\})\rangle$ for holes on the B sublattice, the operators in Eq. (7) should be interchanged according to Eq. (6). The next step is to build Bloch wavefunctions by Fourier transformation of the basis functions Eq. (7). Then the Hamiltonian (5) will be diagonal with respect to \vec{k} -vector. The hopping term of the Hamiltonian \mathcal{H}_{el} couples the $|\Psi^A(\ell, \{p\})\rangle$ and $|\Psi^B(\ell', \{p\})\rangle$ -wavefunctions on the neighboring sites. The vibrational wavefunctions give a product of Huang-Rhys factors, but a shared oxygen contributes a non-factorizable overlap integral. However if one treats this shared oxygen as two independent atoms, one coupled to each site, then the Hamiltonian has a simple form:

$$\begin{aligned} \mathcal{H}_{pp'}^{\text{AA}}(\vec{k}) &= \mathcal{H}_{pp'}^{\text{BB}}(\vec{k}) = \delta_{\{p\}\{p'\}} \left[\frac{\Delta}{4} + \sum_{\alpha} (p_{+\alpha} + p_{-\alpha}) \right] \\ \mathcal{H}_{pp'}^{\text{AB}}(\vec{k}) &= \mathcal{H}_{pp'}^{\text{BA}}(\vec{k}) = \varepsilon(\vec{k}) \prod_{\alpha} (-1)^{p_{+\alpha} + p'_{-\alpha}} \\ &\left[P(p_{+\alpha}, \kappa_{\alpha}) P(p_{-\alpha}, \kappa_{\alpha}) P(p'_{+\alpha}, \kappa_{\alpha}) P(p'_{-\alpha}, \kappa_{\alpha}) \right]^{1/2}, \quad (8) \end{aligned}$$

where $P(p, \kappa) = \exp(-\kappa^2) \kappa^{2p} / p!$ is a Poisson distribution. Since off-diagonal terms factorize, the analytical solution is available in this approximation:

$$\begin{aligned} \Psi_{\lambda}^{1,2}(\vec{k}) &= \sum_{\{p\}=0}^{\infty} \prod_{\alpha} (-1)^{p_{-\alpha}} \left[P(p_{+\alpha}, \kappa_{\alpha}) P(p_{-\alpha}, \kappa_{\alpha}) \right]^{1/2} \\ &\frac{\Psi_{\vec{k}}^A(\{p\}) \pm \Psi_{\vec{k}}^B(\{p\})}{\sqrt{2G'(x_{\lambda})} (\sum_{\alpha'} (p_{+\alpha'} + p_{-\alpha'}) - x_{\lambda})}. \quad (9) \end{aligned}$$

The corresponding eigenvalues are:

$$\begin{aligned} E_{\lambda}^{1,2}(\vec{k}) &= \frac{\Delta}{4} + x_{\lambda}^{1,2}(\vec{k}), \quad 1 + \varepsilon_{1,2}(\vec{k}) G(x_{\lambda}^{1,2}) = 0 \\ G(x_{\lambda}) &= e^{-3\Delta/4} \sum_{p=0}^{\infty} \frac{(3\Delta/4)^p}{p!} \frac{1}{p - x_{\lambda}}. \quad (10) \end{aligned}$$

The $G'(x_{\lambda})$ function in Eq. (9) is a first derivative of $G(x_{\lambda})$ and makes wavefunctions normalized. The correct solution needs a numerical diagonalization of the Hamiltonian which explicitly includes vibrational states of the four shared oxygens. As can be seen on Fig. 2 the difference is negligible between a typical spectrum obtained using approximation (10) and correct numerical treatment. The ground state of the Hamiltonian (8), with energy (from Eq. 10) $E_0(\vec{k}) = \Delta/4 + x_0(\vec{k})$, corresponds

to the anti-JT polaron. Its effective mass, deduced from $d^2 x_0(\vec{k}) / d\vec{k}^2$, provides a realistic alternative (exact for $\Delta \rightarrow 0$ or ∞) to the available variational approaches [18] or exact quantum Monte Carlo simulations [19].

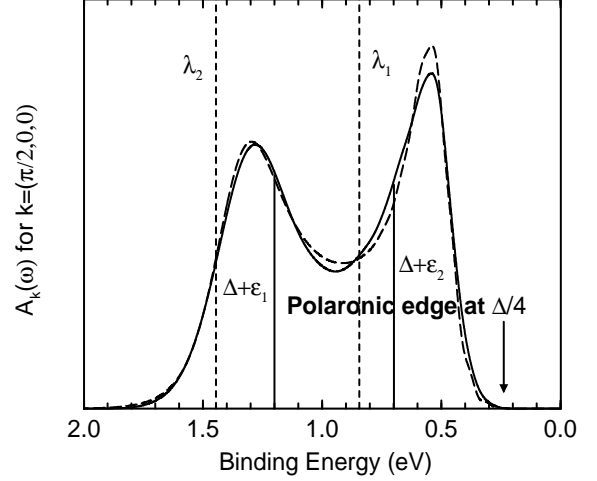


FIG. 2. Energy dependence of the imaginary part of the Green function at $T=0$ and $\vec{k} = (\pi/2, 0, 0)$. The solid line is numerical diagonalization of (5) in the subspace (7). The long-dashed line is the analytical approximation (10) and (12). The spectral function consists of two asymmetric peaks with mean values $\Delta + \varepsilon_{1,2}$. The zero-phonon line is seen at the adiabatic ground state polaron energy $\Delta/4$ [9]. The dashed lines show the peak positions $\lambda_{1,2}$ of the uncorrelated electron theory Eq. (3).

An ARPES experiment measures the spectral function $A(\vec{k}, \omega) = -\frac{1}{\pi} G(\vec{k}, \omega)$ with momentum \vec{k} fully resolved, provided there is no dispersion in the direction perpendicular to the surface. Although LaMnO_3 is cubic, because of the layered AFA magnetic structure, at low temperatures Mn e_g electrons are two-dimensional and the spectrum can be measured:

$$A(\vec{k}, \omega) = \sum_f | \langle f | d^\dagger(\vec{k}) | \text{GS}, \infty \rangle |^2 \delta(E - E_f). \quad (11)$$

The operator $d^\dagger(\vec{k})$ excites a hole from the JT ground state. Summation over final eigenstates $|f\rangle$ includes summation over branch index $i = 1, 2$ and number of phonons $\lambda = 0, 1, \dots, \infty$. The sequence of delta functions in Eq. (11) should be replaced by convolved local densities of phonon states, which we approximate by a Gaussian, $\delta(E) \rightarrow \exp(-E^2/2\gamma^2) / \sqrt{2\pi}\gamma$. Substituting solution (9), (10) into equation (11), we obtain the spectral function:

$$A(\vec{k}, \omega) = \sum_{\lambda, i} \frac{G^2(x_{\lambda}^i)}{G'(x_{\lambda})} \delta(E - E_{\lambda}^i). \quad (12)$$

Equation (12) along with (10) gives the ARPES spectrum normalized to $\int d\omega A(\vec{k}, \omega) = 1$. The first energy moment of the spectrum [17] coincides with the free hole

energy calculated in the “frozen” lattice approximation $\Delta + \varepsilon_{1,2}(\vec{k})$ shown on Fig. 2. The edge of the spectrum corresponds to polaron creation at energy $\approx \Delta/4$. This transition is weaker by 3 orders of magnitude than the peak at $\approx \Delta + \varepsilon_{1,2}(\vec{k})$.

At room temperature magnetic order is lost. The paramagnetic state is modeled by a mean field approximation, namely scaling the effective hopping integral by 2/3 and allowing hopping in $\pm\hat{z}$ direction. This modifies the single particle energy band entering Eq. (8) to $\varepsilon_{1,2}(\vec{k}) = t/3(-2C_z \pm (C_x + C_y))$. But the JT orbital order is not destroyed at T=300 K and Franck-Condon broadening is still expected. When spins are disordered, \vec{k} is not a good quantum number and additional broadening is expected. Only phonon broadening of the ARPES along with peak positions are shown on Fig. 1(b).

The angle-integrated spectrum, shown on Fig. 3 for low and high temperatures, has a width of about 1.2 eV and is almost temperature independent. The uncorrelated (U=0) band structure, shown for comparison, is sensitive to magnetic order and therefore temperature dependent.

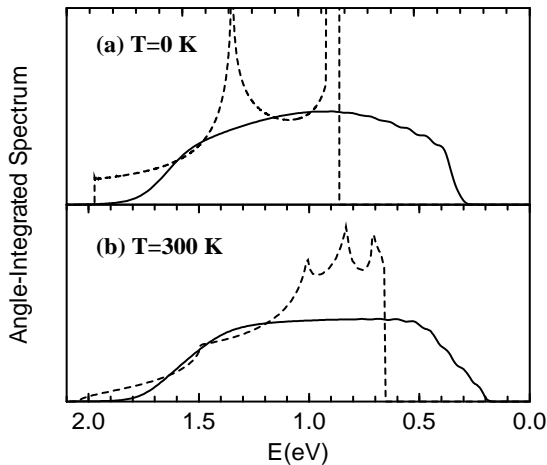


FIG. 3. Angle-integrated photoemission spectrum (solid line) at (a) T=0 K and (b) T=300K. At room temperature, spins are disordered, but JT order is not destroyed. For comparison, the uncorrelated electron (U=0 limit) band structure density of states is shown by the dashed lines, with 2D Van Hove singularities at T=0 K.

The existing photoemission data [5,6] are consistent with our predictions. Higher resolution experiments are needed to test the theory and to unravel the nature of the lowest energy excitations in the LaMnO₃. To make such an experiment possible, a single domain sample (having 2D dispersion at T=0K) is needed, with good control of oxygen concentration [20].

ACKNOWLEDGMENTS

We thank P. D. Johnson for helpful conversations. This work was supported in part by NSF Grant No. DMR-9725037.

-
- [1] R. M. Kusters, J. Singleton, D. A. Keen, R. McGreevy, and W. Hayes, *Physica B* **155**, 362 (1989); S. Jin, T. H. Tiefel, M. McCormack, R. A. Fastnacht, R. Ramesh, and L. H. Chen, *Science* **264**, 413 (1994).
 - [2] *Colossal Magnetoresistance, Charge Ordering, and Related Properties of Manganese Oxides*, edited by C.N.R. Rao and B. Raveau (World Scientific, Singapore, 1998).
 - [3] J. Rodriguez-Carvajal, M. Hennion, F. Moussa, A. H. Moudden, L. Pinsard, and A. Revcolevschi, *Phys. Rev. B* **57**, 3189 (1998).
 - [4] Y. Murakami, J. P. Hill, D. Gibbs, M. Blume, I. Koyama, M. Tanaka, H. Kawata, T. Arima, Y. Tokura, K. Hirota, and Y. Endoh, *Phys. Rev. Lett.* **81**, 582 (1998).
 - [5] J. H. Park, C. T. Chen, S. W. Cheong, W. Bao, G. Meigs, V. Chakarian and Y. U. Idzerda, *Phys. Rev. Lett.* **76**, 4215 (1996); T. Saitoh, A. E. Bocquet, T. Mizokawa, H. Namatame and A. Fujimori, *Phys. Rev. B* **51**, 13942 (1995).
 - [6] D. S. Dessau and Z. X. Shen, in *Colossal Magnetoresistive Oxides*, edited by Y. Tokura (World Scientific, Singapore, 1998).
 - [7] W. E. Pickett and D. Singh, *Phys. Rev. B* **53**, 1146 (1996); S. Satpathy, Z. S. Popović and F. R. Vukajlović, *Phys. Rev. Lett.* **76**, 960 (1996); I. Solovyev, N. Hamada and K. Terakura, *Phys. Rev. Lett.* **76**, 4825 (1996); Y.-S. Su, T. A. Kaplan, S. D. Mahanti and J. F. Harrison, *Phys. Rev. B* **61**, 1324 (2000).
 - [8] J. Kanamori, *J. Appl. Phys.* **31**, 14S (1960); K. I. Kugel and D. I. Khomskii, *Sov. Phys. Usp.* **25**, 231 (1982).
 - [9] P. B. Allen and V. Perebeinos, *Phys. Rev. B* **60**, 10747 (1999).
 - [10] F. J. Himpsel, N. Schwentner, E. E. Koch, *Phys. Status Solidi B* **71**, 615 (1975).
 - [11] G. A. Sawatzky, *Nature* **342**, 480 (1989).
 - [12] A. J. Millis, *Phys. Rev. B* **53**, 8434 (1996).
 - [13] J. C. Slater and G. F. Koster, *Phys. Rev.* **94**, 1498 (1954).
 - [14] J. H. Jung, K. H. Kim, D. J. Eom, T. W. Noh, E. J. Choi, J. Yu, Y. S. Kwon, and Y. Chung, *Phys. Rev. B* **55**, 15489 (1997); J. H. Jung, K. H. Kim, T. W. Noh, E. J. Choi, and J. Yu, *Phys. Rev. B* **57**, 11043 (1998).
 - [15] P. B. Allen and V. Perebeinos, *Phys. Rev. Lett.* **83**, 4828 (1999).
 - [16] M. N. Iliev, M. V. Abrashev, H.-G. Lee, V. N. Popov, Y. Y. Sun, C. Thomsen, R. L. Meng, and C. W. Chu, *Phys. Rev. B* **57**, 2872 (1998); V. B. Podobodov, A. Weber, D. Romero, J. P. Rice and H. D. Drew, *Phys. Rev. B* **58**, 43 (1998).
 - [17] K. Cho and Y. Toyozawa, *J. Phys. Soc. Jpn.* **30**, 1555 (1971).

- [18] A. H. Romero, D. W. Brown and K. Lindenberg, Phys. Rev. B **59**, 13728 (1999).
- [19] P. E. Kornilovitch, Phys. Rev. Lett. **84**, 1551 (2000).
- [20] B. Dabrowski, R. Dybziński, Z. Bukowski, O. Chmaissem, J. D. Jorgensen, J. Solid State Chem. **146**, 448 (1999).